Direct Observation of the Protonation States in the Mutant Green Fluorescent Protein

Chie Shibazaki, † Rumi Shimizu, † Yuji Kagotani, † Andreas Ostermann, § Tobias E. Schrader, ‡ Motoyasu Adachi,, †*

† Institute for Quantum Life Science, National Institutes for Quantum and Radiological Science and Technology (QST), 2-4 Shirakata, Tokai, Ibaraki, 319-1106, Japan

§ Heinz Maier-Leibnitz Zentrum (MLZ), Technische Universität München, Lichtenbergstr. 1, 85748 Garching, Germany

‡ Jülich Centre for Neutron Science (JCNS) at Heinz Maier-Leibnitz Zentrum (MLZ), Forschungszentrum Jülich GmbH, Lichtenbergstrasse 1, 85748 Garching, Germany

Corresponding Author

*E-mail: adachi.motoyasu@qst.go.jp (M.A.).

ABSTRACT

Neutron crystallography has been used to elucidate the protonation states for the enhanced green fluorescent protein, which has revolutionized the imaging technologies. The structure has a deprotonated hydroxyl group in the fluorescent chromophore. Also, the protonation states of His148 and Thr203, as well as the orientation of a critical water molecule in direct contact with the chromophore, could be determined. The results demonstrate that the deprotonated hydroxyl group in the chromophore and the nitrogen atom ND1 in His148 are charged negatively and positively, respectively, forming an ion pair. The position of the two deuterium atoms in the critical water molecule appears to be displaced slightly toward the acceptor oxygen atoms according to their omit maps. This displacement implies the formation of an intriguing electrostatic potential realized inside the protein. Our findings provide new insights into future protein design strategies along with developments in quantum chemical calculations.

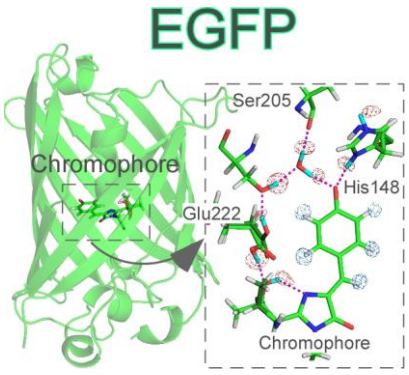

KEYWORDS neutron diffraction, GFP, water molecule, chromophore, hydronium ion

TEXT.

Fluorescent proteins (FPs) have revolutionized the imaging technologies in biological science, and the green fluorescent protein (GFP) is one of the key FPs as a representative and pioneer molecule.[1–5] The isolation of not only GFP but also other FPs and their protein engineering have provided the coloring diversity with additional functions such as photoswitching leading to super-resolution microscopy.[6,7] A better understanding of the structure and function for FPs will help to develop new molecular designs to generate further practical devices. Here, we report direct evidence to show the characteristic protonation (deuteration) states of the chromophore and surrounding key residues with their hydrogen-bonding network, including water molecules, by neutron crystallography.

The recombinant GFP used in this study, named as EGFPq, includes mutations of C48S, F64L, S65T, Q80R, N159Q, and I167T with two and seven amino acid deletions at N- and C-terminals, respectively, when compared to the original sequence[8] (Figure S1 and S2). The mutations F64L and S65T correspond to the enhanced green fluorescent protein (GFPmut1, EGFP).[9–12] The other mutations were introduced to improve chemical protein stability and crystal packing. The hydrogenated EGFPq was purified and crystallized into a crystal volume of about 1.7 mm^3 for neutron crystallography (Materials and Methods in supporting information, Figure S3). The mother liquor solution of the crystal was exchanged against a corresponding deuterated solution for a replacement of exchangeable hydrogen atoms to deuterium atoms. The replacement of the mother-liquor decreases the background generated by the incoherent scattering contribution of the hydrogen atoms and improves structural analysis because of the higher and positive neutron scattering length of deuterium compared to hydrogen.[13] Neutron diffraction data were collected to 1.45 Å resolution using the neutron diffractometer BioDiff[14]

installed at the Forschungs-Neutronenquelle Heinz Maier-Leibnitz FRM II (Garching, Germany) with a wavelength of 2.668 Å at 100 K. X-ray diffraction data were collected to 0.88 Å resolution at beamline BL5A at the High Energy Accelerator Research Organization KEK Photon Factory (Tsukuba, Japan). The crystal structure of EGFPq was refined by a joint refinement module in the program Phenix[15] to an R-factor of 16.8% and a free R-factor of 20.7% of the neutron diffraction data and an R-factor of 15.4% and free R-factor of 16.5% for X-ray diffraction (Table S1). The overall structure is shown in Figure S4. One asymmetric unit includes one EGFPq molecule comprising 228 residues, two sulfate ions, and 381 heavy water molecules. The crystal packing corresponds to those reported previously.[10,16–18]

The first remarkable engineering to GFP is the single point mutation S65T.[9,10] The beneficial point mutation of F64L increases the folding efficiency of GFP at 37 °C.[11,12] These mutations result in increased fluorescence, photostability, a shift of the major excitation peak, and keeps the emission peak around 510 nm as EGFP. Although EGFPq used in this study includes additional mutations for improved crystal packing, it corresponds to EGFP, as indicated by its spectrum shown in Figure S5. Figure 1A shows the structure of the chromophore and its surrounding residues with hydrogen and deuterium atoms visualized by neutron crystallography. Analysis of the neutron scattering lengths density maps indicates that the OH atom of the chromophore is not protonated, while the corresponding oxygen atom in the switching chromogenic protein Dathail is protonated according to the structure determined by neutron crystallography.[19] In EGFPq, the deuterium atoms DD1 in His148, DG1 in Thr203, and D2 in DOD323 were assigned around the OH oxygen atom of the chromophore based on omit maps. These deuterium atoms are involved in strong hydrogen bonds with the bond lengths of 2.78, 2.70, and 2.70 Å, respectively, between the hydrogen donor and acceptor atoms. These results

demonstrate that the OH oxygen atom in the chromophore is deprotonated and, therefore, exists in its anion form consistent with previous results.[18, 20, 21] Figure 1B and Table S2 show the atom names and bond lengths in the chromophore. The bond length between CZ and OH is slightly shortened compared to those of the A-type (PDBID: 6JGH)[18], in which the chromophore is protonated. The bond length between CA2 and CB2 is shorter than that between CB2 and CG2. The differences in the bond lengths are consistent with the state of the negatively charged OH oxygen atom. Probably, this is caused by the difference of resonance structure between EGFPq and GFPq (the T65S derivative of EGFPq as shown in Figure S2).

The two deuterium atoms DE2 and DD1 in His148 are modeled on the omit maps obtained by neutron crystallography and are shown in Figure 1A and Figure S6. This configuration represents the double protonation of His148, as were observed in electron density maps by previous X-ray analysis.[18] Interestingly, the DE2 atom in its imidazole ring seems to be located as a tetrahedral configuration of the NE2 atom rather than sp2 configuration. Probably, the two double bonds in imidazole ring are localized as shown in Figure S6C, which indicates that the ND1 atom could have a positive charge. The configuration of the NE2 atom must be advantageous for the negative charge of the OH group in the chromophore. It appears that the amid D atom in the main chain of Arg168 donates a hydrogen atom to the NE2 atom in His148 with a distance of 3.14 Å between the hydrogen donor and acceptor atoms. The planar conformation of NE2 in His148 will be not satisfied because of the steric hindrance between DE2 in His148 and D in Arg168. Assuming that the DE2 atom in His148 is positioned in the plane of the imidazole ring, the distance to the D atom in Arg168 would be 1.40 Å. According to the unrestrained refinement in this study, the position of the DE2 atom in His148 was located at a distance of 0.42 Å from the position of the restraint refinement. The location seems to dissolve

the steric hindrance against the amid D atom of Arg168, although the tetrahedral conformation is slightly distorted. To discuss the accurate position of the nuclei of the DE2 atom, higher-resolution analysis and explicit quantum chemical calculations should be performed.

DOD323 and the hydroxyl group of Ser205 are positioned between the OH atom of the chromophore and the side chain of Glu222 in the hydrogen bonding network responsible for an excited proton transfer in GFP.[22–24] In this analysis, we observed two hydrogen bonds based on omit maps of the D1 atom in DOD323 and the DG atom in Ser205. The first bond was between the O atom in DOD323 and the OG atom in Ser205, and the second was between the O atom in DOD323 and the O atom in Asn146. Notably, the position of the two deuterium atoms in DOD323 appears to be displaced slightly to the acceptor oxygen atoms according to their omit maps (Figure2). In reality, the differences seem to be significant when compared to the sigma value estimated from the refinement (Table S3) and those of the bond distances in other water molecules which have lower thermal factors (Figure S7). An unrestrained refinement, which introduced a slack value for the bond length to make a square well potential, showed the movement of D1 and D2 to the acceptor O atoms in Asn146 and OH in the chromophore with a distance of 0.14 and 0.18 Å, respectively (Figure2 and Table S3). This refinement was similar to the result observed in protein kinase.[25] The length of the OH bond interacting with the oxygen acceptor atom correlated to the pKa value between the two groups and could form single-well potential with similar pKa values.[26] However, a shared proton was reported in the photoactive yellow protein despite different pKa values of about 4.5 units.[27] Also, the displacement seems to depend on pH.[28] The displaced position of the deuterium atoms in the water molecule of DOD323 might imply the formation of an intriguing electrostatic potential surface realized inside

the protein, a large and complicated molecule. Our findings will provide new insights into future protein design strategies along with developments in quantum chemical calculations.

We found a hydronium ion on the molecular surface, as shown in Figure 3 and similar to previous examples.[29–31] The hydronium ion was positioned near protonated Glu17 on a proton antenna at the negative potential surface of GFP.[16] Whereas the seven deuterium atoms of DOD322, DOD336, and Glu17 including D1 and D3 atoms in D3O300 were observed by the omit maps, the D2 atom of the hydronium ion seems to be located near the center between the two oxygen atoms of DOD336 and the hydronium ion similar to a delocalized form ([H2O···H···OH2]+). The negative electrostatic potential should affect the protonation of Glu17, the existence of the hydronium ion, and the configuration of deuterium atoms.

The residue Glu222 and the chromophore in wild-type GFP have been postulated to be deprotonated and protonated, respectively. In contrast, the residue Glu222 and the chromophore in the S65T mutant of GFP are protonated and deprotonated, respectively. These findings correspond to the two states resulting in the excited proton transfer through the hydrogen bonding network between Glu222 and the chromophore in wild-type GFP.[23,24] One of the questions is why the mutation S65T generates protonation for Glu222 and deprotonation for the chromophore. In this analysis of EGFPq, the protonated form of Glu222 and a part of the chromophore derived from the residue Thr65 are observed in alternative conformations (Figure 1A). The alternative form A makes two hydrogen bonds between the OE2 atom in Glu222 and the OG1 atom in the chromophore, and between OG1 and the N2 atom in chromophore.

In contrast, Glu222 forms a hydrogen bond with Ser205 without interacting with the chromophore in the alternative form B. These hydrogen bonding networks cannot account for the

deprotonation mechanism of the chromophore in EGFP, because the alternative conformations of Glu222 are similar between GFP and EGFP derivatives.[17] We should focus on the environment of the OH group in the chromophore. Figure 4 compares structure of EGFPq with GFPq. One can observe a different conformation for His148 and a slightly different position for the OH atom of the chromophore. The alternative structure of His148 in GFPq is consistent with the separation of spectrum peaks as shown in Figure S5, and its dynamics might display key roles for protonation of the chromophore at acidic pH conditions and proton transfer with bulk solvent in the mutant GFPs.[32,33] However, this site does not interact with the S65T mutation site directly. One explanation for the differences could be that the steric hindrance of Leu220 with the methyl group of CG2 in the chromophore affects the structure of the strand, including Asn146 and His148, which directly interacts with DOD323 and the OH atom in the chromophore, via Tyr145 and Leu207. The protonation mechanisms of His148 in EGFP might be determined by structural arrangements at the molecular level. Further mutation analyses are currently been performed to understand the fascinating mechanism observed in the mutant engineered at early stage.

Experimental Methods

Experimental details are described in the supporting information. Briefly, GFP mutant proteins are prepared using an Escherichia coli expression system in insoluble fraction. Proteins were refolded by a dilution method and purified by ion-exchanging column chromatography. For preparation of the large crystal, the precipitant solution containing 0.1 M MES-NaOD (pD 7.0), 5.0 % w/v PEG 2000 and 50 mM NDSB (160 µl) was mixed with 38 mg/ml protein solution in 20 mM Tris-DCl buffer (pD 8.0) containing 1 mM DTT (240 µl), and equilibrated against 4 ml

of the reservoir solution, which was composed of 0.1 M MES–NaOD (pD 7.0), 9.0 % w/v PEG 2000 and 50 mM NDSB at 293K.

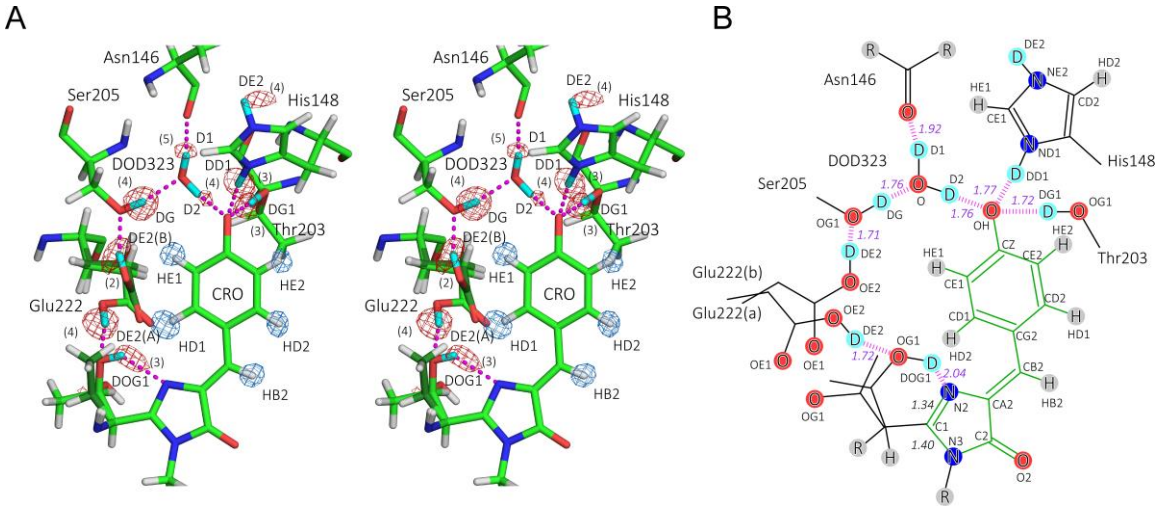

(Please, use double column format)

Figure 1 Neutron crystal structure of the chromophore and interacting residues in EGFPq. (A) Bond model and neutron scattering length density maps of hydrogen and deuterium atoms are represented with a stereo view. Hydrogen (light grey), deuterium (cyan), carbon (green), oxygen (red), nitrogen (blue) atoms are drawn. F_o–F_c neutron omit maps for hydrogen atoms in the chromophore are shown in marine blue at −4.0 σ. F_o–F_c neutron omit maps for deuterium atoms in His148, Glu222, DOD323, and the chromophore are shown in red at the level ranging from 2 to 4 σ. The sigma values are indicated in the parenthesis. Hydrogen bonds are represented with dotted lines in magenta by a unit of Å. (B) Schematic drawing of (A). The atom names and bond distances are shown.

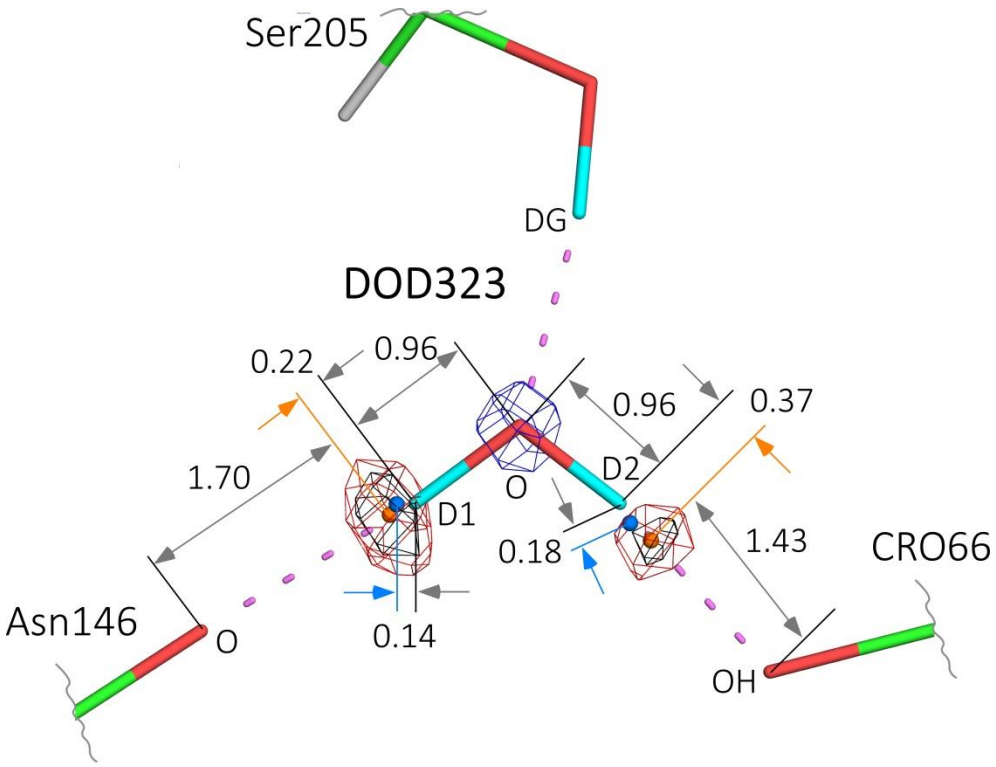

Figure 2 Magnified model of DOD323 with omit maps. F_o–F_c neutron omit maps for D1 and D2 atoms for the DOD323 molecule are shown in red and black at 4.0 and 5.0 σ, respectively. $2F_o$–F_c X-ray map for oxygen atom is shown in blue at 5.0 σ. The marine blue and orange spheres represent the position of deuterium atoms calculated by unrestraint refinement and the center of omit maps, respectively. The distances are indicated in a unit of Å.

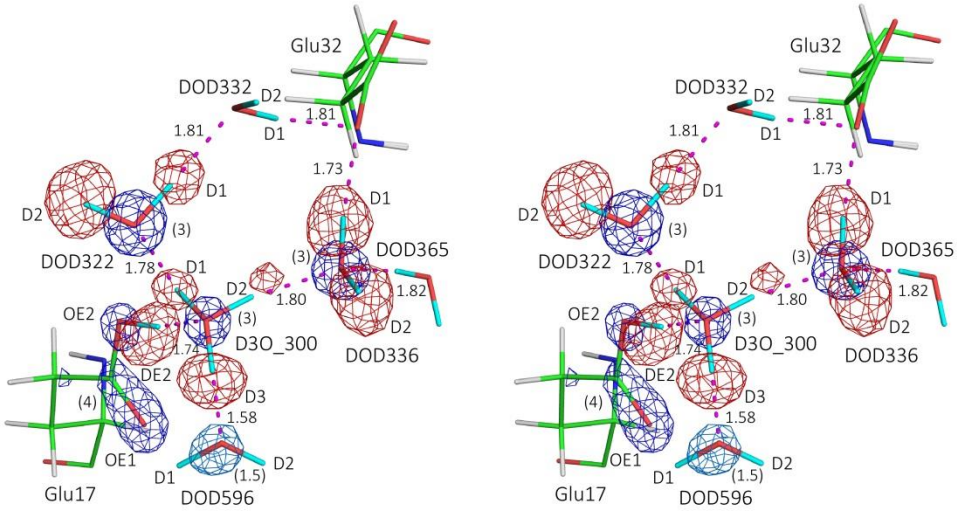

(Please, use double or 1.5 column format)

Figure 3 Hydronium ion modeled near Glu17 on the molecular surface of EGFPq. Fo–Fc neutron omit maps for deuterium are shown in red at a 4 σ level. 2Fo–Fc X-ray electron density maps of the oxygen atoms are shown in blue at a level ranging from 1.5 to 4 σ. The sigma values are indicated in the parenthesis.

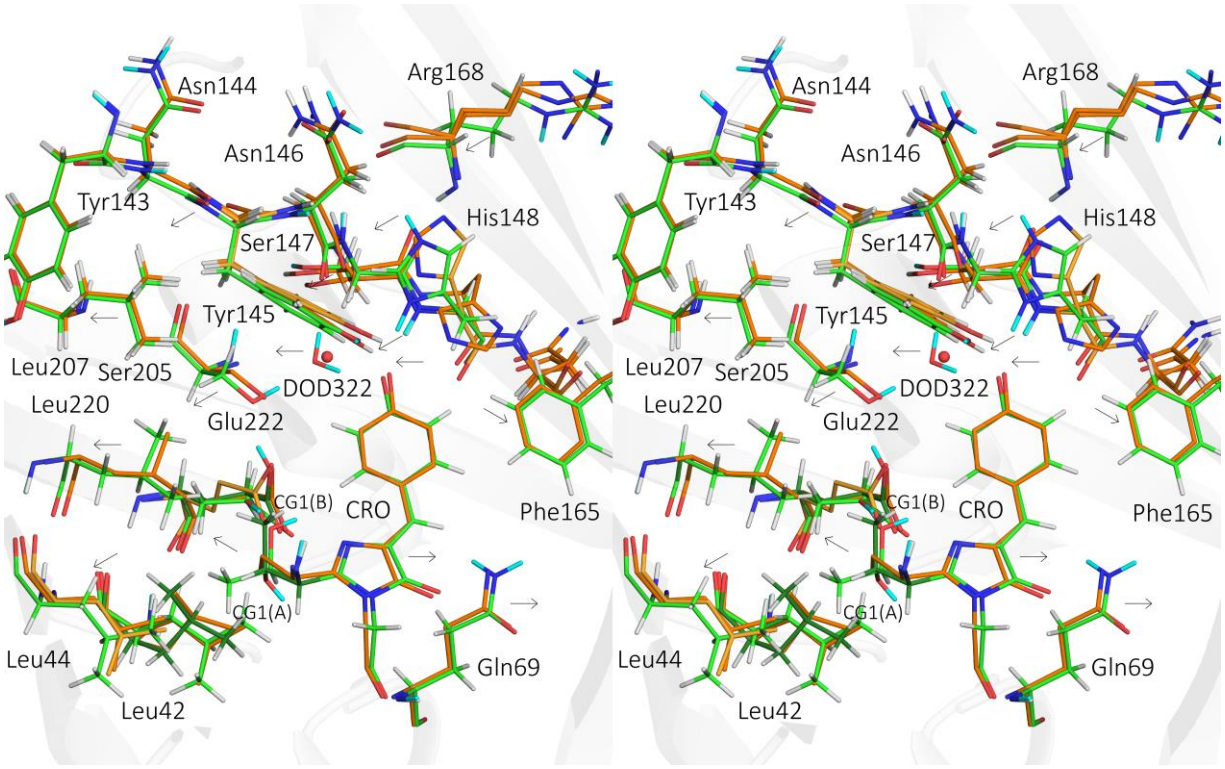

(Please, use double or 1.5 column format)

Figure 4 Superimposition of structural models between EGFPq and GFPq. Carbon atoms for EGFPq and GFPq are shown in green and orange, respectively. The arrows indicate the differences between the two structures.

ASSOCIATED CONTENT

The Supporting Information is available free of charge on the ACS Publications website at DOI:.

Detailed description of construction of expression plasmids; protein expression and purification; preparation of large crystal for neutron crystallography; crystal structure determination; absorption and fluorescent measurements; and supplementary Figures S1−S7 and Table S1−S6(PDF).

AUTHOR INFORMATION

Corresponding Author

*E-mail: adachi.motoyasu@qst.go.jp

ORCID

Andreas Ostermann: 0000-0002-1477-5590

Tobias E. Schrader: 0000-0001-5159-0846

Motoyasu Adachi: 0000-0003-2353-880X

ACKNOWLEDGMENT

The neutron diffraction experiment and the synchrotron radiation experiment were performed at BioDiff of FRM-II (proposal No. 12786) and BL5A of Photon Factory (proposal No. 2016G516), respectively. This work was supported by JSPS KAKENHI Grant Number JP16KT0063 (to M.A.) and by QST President's Strategic Grant (Exploratory Research) (to R.S.), and partially supported Diversity Promotion Office in QST and by J-PARC MLF deuteration laboratory.

REFERENCES

(1) Shimomura, O.; Johnson, F. H.; Saiga, Y. Extraction, purification and properties of aequorin, a bioluminescent protein from the luminous hydromedusan, Aequorea. *J. Cell Comp. Phys.* **1962**, *59*, 223-239.

(2) Tsien, R. Y. The green fluorescent protein. *Annu. Rev. Biochem.* **1998**, *67*, 509-544.

(3) Sanders, J. K.; Jackson, S. E. The discovery and development of the green fluorescent protein, GFP. *Chem. Soc. Rev.* **2009**, *38*(10), 2821-2822.

(4) Chudakov, D. M.; Matz, M. V; Lukyanov, S.; Lukyanov, K. Fluorescent proteins and their applications in imaging living cells and tissues. *Physiol. Rev.* **2010**, *90*(3), 1103-1163.

(5) Acharya, A.; Bogdanov, A. M.; Grigorenko, B. L.; Bravaya, K. B.; Nemukhin, A. V.; Lukyanov, K. A.; Krylov, A. I. Photoinduced Chemistry in Fluorescent Proteins: Curse or Blessing? *Chem. Rev.* **2017**, *117*(2), 758-795.

(6) Nienhaus, K.; Nienhaus, G. U. Fluorescent proteins for live-cell imaging with super-resolution. *Chem. Soc. Rev.* **2014**, *43*(4), 1088-1106.

(7) Storti, B.; Margheritis, E.; Abbandonato, G.; Domenichini, G.; Dreier, J.; Testa, I.; Garau, G.; Nifosì, R.; Bizzarri, R. Role of Gln222 in Photoswitching of Aequorea Fluorescent Proteins: A Twisting and H-Bonding Affair? *ACS Chem. Biol.* **2018**, *13*(8), 2082-2093.

(8) Prasher, D. C.; Eckenrode, V. K.; Ward, W. W.; Prendergast, F. G.; Cormier, M. J. Primary structure of the *Aequorea victoria* green-fluorescent protein. *Gene* **1992**, *111*(2), 229-233.

(9) Cubitt, A. B.; Heim, R.; Adams, S. R.; Boyd, A. E.; Gross, L. A.; Tsien, R. Y. Understanding, improving and using green fluorescent proteins. *Trends Biochem. Sci.* **1995**, *20*(11), 448-455.

(10) Ormö, M.; Cubitt, A. B.; Kallio, K.; Gross, L. A.; Tsien, R. Y.; Remington, S. J. Crystal structure of the *Aequorea victoria* green fluorescent protein. *Science* **1996**, *273*(5280), 1392-1395.

(11) Cormack, B. P.; Valdivia, R. H.; Falkow, S. FACS-optimized mutants of the green fluorescent protein (GFP). *Gene* **1996**, *173*, 33-38.

(12) Yang, T. T.; Cheng, L.; Kain, S. R. Optimized codon usage and chromophore mutations provide enhanced sensitivity with the green fluorescent protein. *Nucleic Acids Res.* **1996**, *24*, 4592-4593.

(13) Oksanen, E.; Chen, J. C.; Fisher, S. Z. Neutron Crystallography for the Study of Hydrogen Bonds in Macromolecules. *Molecules* **2017**, *22*(4), E596.

(14) Heinz Maier-Leibnitz Zentrum et al. BIODIFF: Diffractometer for large unit cells. *Journal of large-scale research facilities* **2015**, *1*: A2.

(15) Adams. P. D.; Afonine. P. V.; Bunkóczi. G.; Chen. V. B.; Davis. I. W.; Echols. N.; Headd. J. J.; Hung. L. W.; Kapral. G. J.; Grosse-Kunstleve. R. W.; McCoy. A. J.; Moriarty. N. W.; Oeffner. R.; Read. R. J.; Richardson. D. C.; Richardson. J. S.; Terwilliger. T. C.; Zwart. P. H. PHENIX: a comprehensive Python-based system for macromolecular structure solution. *Acta Crystallogr.* D **2010**, *66*(Pt 2), 213-221.

(16) Shinobu, A.; Palm, G. J.; Schierbeek, A. J.; Agmon, N. Visualizing proton antenna in a high-resolution green fluorescent protein structure. *J. Am. Chem. Soc.* **2010**, *132*(32), 11093-11102.

(17) Arpino, J. A.; Rizkallah, P. J; Jones, D. D. Crystal structure of enhanced green fluorescent protein to 1.35 Å resolution reveals alternative conformations for Glu222. *PLoS One* **2012**, *7*(10), e47132.

(18) Takaba. K.; Tai. Y.; Eki. H.; Dao. H. A.; Hanazono. Y.; Hasegawa. K.; Miki. K.; Takeda. K. Subatomic resolution X-ray structures of green fluorescent protein. *IUCrJ.* **2019**, *6*(Pt 3), 387-400.

(19) Langan, P. S.; Close, D. W.; Coates, L.; Rocha, R. C.; Ghosh, K.; Kiss, C.; Waldo, G.; Freyer, J.; Kovalevsky, A.; Bradbury, A. R. Evolution and characterization of a new reversibly photoswitching chromogenic protein, Dathail. *J. Mol. Biol.* **2016**, *428*, 1776-1789.

(20) Brejc, K.; Sixma, T. K.; Kitts, P. A.; Kain, S. R.; Tsien, R. Y.; Ormö, M.; Remington, S. J. Structural basis for dual excitation and photoisomerization of the *Aequorea victoria* green fluorescent protein. *Proc. Natl. Acad. Sci. U. S. A.* **1997**, *94*(6), 2306-2311.

(21) Elsliger, M. A.; Wachter, R. M.; Hanson, G. T.; Kallio, K.; Remington, S. J. Structural and spectral response of green fluorescent protein variants to changes in pH. *Biochemistry* **1999**, *38*(17), 5296-5301.

(22) Meech, S. R. Excited state reactions in fluorescent proteins. *Chem. Soc. Rev.* **2009**, *38*(10), 2922-2934.

(23) Grigorenko, B. L.; Nemukhin, A. V.; Polyakov, I. V.; Morozov, D. I.; Krylov, A. I. First-principles characterization of the energy landscape and optical spectra of green fluorescent protein along the A→I→B proton transfer route. *J. Am. Chem. Soc.* **2013**, *135*(31), 11541-11549.

(24) Laptenok, S. P.; Lukacs, A.; Gil, A.; Brust, R.; Sazanovich, I. V.; Greetham, G. M.; Tonge, P. J.; Meech, S. R. Complete Proton Transfer Cycle in GFP and Its T203V and S205V Mutants. *Angew. Chem. Int. Ed. Engl.* **2015**, *54*(32), 9303-9307.

(25) Shibazaki, C.; Arai, S.; Shimizu, R.; Saeki, M.; Kinoshita, T.; Ostermann, A.; Schrader, T. E.; Kurosaki, Y.; Sunami, T.; Kuroki, R.; Adachi, M. Hydration Structures of the Human Protein Kinase CK2α Clarified by Joint Neutron and X-ray Crystallography. *J. Mol. Biol.* **2018**, *430*(24), 5094-5104.

(26) Sigala, P. A.; Ruben, E. A.; Liu, C. W.; Piccoli, P. M.; Hohenstein, E. G.; Martínez, T. J.; Schultz, A. J.; Herschlag, D. Determination of Hydrogen Bond Structure in Water versus Aprotic Environments To Test the Relationship Between Length and Stability. *J. Am. Chem. Soc.* **2015**, *137*(17), 5730-5740.

(27) Yamaguchi, S.; Kamikubo, H.; Kurihara, K.; Kuroki, R.; Niimura, N.; Shimizu, N.; Yamazaki, Y.; Kataoka, M. Low-barrier hydrogen bond in photoactive yellow protein. *Proc. Natl. Acad. Sci. U. S. A.* **2009**, *106*(2), 440-444.

(28) Gerlits, O.; Wymore, T.; Das, A.; Shen, C. H.; Parks, J. M.; Smith, J. C.; Weiss, K. L.; Keen, D. A.; Blakeley, M. P.; Louis, J. M.; Langan, P.; Weber, I. T.; Kovalevsky, A. Long-Range Electrostatics-Induced Two-Proton Transfer Captured by Neutron Crystallography in an Enzyme Catalytic Site. *Angew. Chem. Int. Ed. Engl.* **2016**, *55*(16), 4924-4927.

(29) Kovalevsky, A. Y.; Hanson, B. L.; Mason, S. A.; Yoshida, T.; Fisher, S. Z.; Mustyakimov, M.; Forsyth, V. T.; Blakeley, M. P.; Keen, D. A.; Langan, P. Identification of the elusive hydronium ion exchanging roles with a proton in an enzyme at lower pH values. *Angew. Chem. Int. Ed. Engl.* **2011**, *50*(33), 7520-7523.

(30) Cuypers, M. G.; Mason, S. A.; Blakeley, M. P.; Mitchell, E. P.; Haertlein, M.; Forsyth, V. T. Near-atomic resolution neutron crystallography on perdeuterated *Pyrococcus furiosus* rubredoxin: implication of hydronium ions and protonation state equilibria in redox changes. *Angew. Chem. Int. Ed. Engl.* **2013**, *52*(3), 1022-1025.

(31) Unno, M.; Ishikawa-Suto, K.; Kusaka, K.; Tamada, T.; Hagiwara, Y.; Sugishima, M.; Wada, K.; Yamada, T.; Tomoyori, K.; Hosoya, T.; Tanaka, I.; Niimura, N.; Kuroki, R.; Inaka, K.; Ishihara, M.; Fukuyama, K. Insights into the Proton Transfer Mechanism of a Bilin Reductase PcyA Following Neutron Crystallography. *J. Am. Chem. Soc.* **2015**, *137*(16), 5452-5460.

(32) Shinobu, A.; Agmon, N. Proton Wire Dynamics in the Green Fluorescent Protein. *J. Chem. Theory Comput.* **2017,** 13(1), 353-369.

(33) Abbruzzetti, S.; Grandi, E.; Viappiani, C.; Bologna, S.; Campanini, B.; Raboni, S.; Bettati, S.; Mozzarelli.; A. Kinetics of acid-induced spectral changes in the GFPmut2 chromophore. *J. Am. Chem. Soc.* **2005,** 127(2), 626-635.